9

Centrifugal, One-Way, and Detent Clutches

These are special-purpose clutches that are used in automatic transmissions, in devices for bringing high-speed machinery up to speed, in chain saws, in conveyor drives, and in similar industrial, vehicular, and large- and small-equipment applications. The centrifugal clutches provide a speed-dependent torque which acts only when the rotational speed exceeds a particular value; the one-way, or overrunning, clutches provide a torque that is not speed dependent once they are engaged, but is dependent on the direction of rotation; and the detent clutches provide a torque that cannot exceed a prescribed value.

I. CENTRIFUGAL CLUTCHES

A centrifugal clutch may be described as consisting of an inner cylinder that is attached to the input shaft and an outer housing that is attached to the output shaft, as in Figure 1. Sectors of the inner cylinder are cut out to allow it to be fitted with weights that can slide radially outward as the inner cylinder rotates so that the weights are forced against the outer housing by centrifugal force and thereby transmit torque to the outer housing. Centrifugal clutches designed for lower power transfer may use simpler designs. In some chain saws, for example, it is the weights themselves that are recessed to accept radial guides from the central shaft.

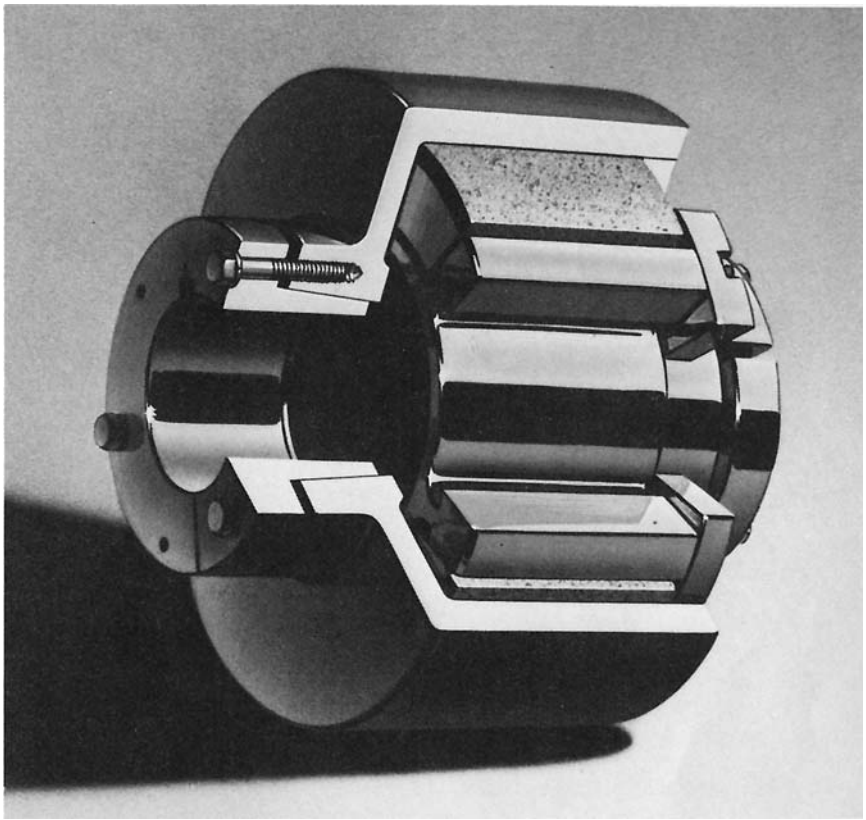

FIGURE 1 Centrifugal clutch. (Courtesy Dana Corp., Inc., Toledo, OH.)

Because of the variety of centrifugal clutch designs, their analysis will be described in general terms. Let A denote the cross-sectional area of each weight in a plane perpendicular to the axis of rotation, written in the form of an annular sector of angle ϕ_o as

$$A = c\phi_o r_o^2(1 - \beta^2) \tag{1-1}$$

where $\beta = r_i/r_o$. Parameters β and c are factors that may be used to express other cross-sectional areas in this form of equation (1-1). When $\beta = 0$, $c = 1/2$, and $\phi_o = 2\pi$, area A in equation (1-1) becomes that of a disc of radius r_o.

Let w denote the width of each weight, measured in a direction parallel to the axis of rotation, and let γ represent the mass density of the weights. If

the static deflection of a retaining spring attached to each mass is δ_s, then its spring constant k is given by

$$k = \gamma A \frac{wg}{\delta_s} \tag{1-2}$$

in which g is the acceleration of gravity, taken to be 9.8067 m/sec^2, or 32.2 ft/sec^2.

Denote the radius to the center of gravity of each weight by r_c. Then the centrifugal force acting on each weight as it rotates at angular velocity ω about the axis of the clutch and moves outward a distance δ is then given by

$$F = \gamma w A (r_c + \delta)\omega^2 - g\kappa \frac{\delta + \delta_s}{\delta_s} \tag{1-3}$$

where the spring constant may be increased by the factor κ to hold each weight more securely against its stop at low rotational speeds.

Consider a prototype weight as being made from a sector of a thick cylinder whose inner radius is r_i and whose outer radius is r_o. Form the sector by cutting the cylinder to length w, which will be the width of the sector, and then cut the cylinder with two radial planes separated by angle ϕ_o. Retain one of the two sectors that subtend angle ϕ_o as the prototype weight shown in later Figure 3(a). The radius of gyration of this weight about the axis of the original cylinder is given by

$$r_c = \frac{r_o}{\sqrt{2}} \sqrt{1 - \beta^2} \tag{1-4}$$

In order to express the radius of gyration of other geometries in this form, let

$$r_c = \lambda r_o \sqrt{1 - \beta^2} \tag{1-5}$$

The torque that can be delivered by N of these weights after they have moved outward a distance δ to make contact with the inner surface of the housing at radius r_o may be written as

$$T = \mu r_o F = \mu \gamma w r_o N A \left[(r_c + \delta)\omega^2 - g\kappa(1 + \eta) \right] \tag{1-6}$$

where $\eta = \delta/\delta_s$. This relation may be solved for the w required for the clutch to transmit torque T at angular speed ω to get

$$w = \frac{T}{N\mu\gamma\phi_o c r_o^3 (1 - \beta^2) \left[(r_c + \delta)\omega^2 - g\kappa(1 + \eta) \right]} \tag{1-7}$$

Maximum pressure on the lining may be found from

$$F = r_o w \int_{-\phi_o/2}^{\phi_o/2} p \cos\phi\omega = r_o w p_{\max} \int_{-\phi_o/2}^{\phi_o/2} \cos(\phi)^2 d\phi$$
$$= \frac{p_{\max}}{2} r_o w(\phi_o + \sin\phi_o) \tag{1-8}$$

upon using the pressure distribution from equation (1-2) in Chapter 4. Hence,

$$p_{\max} = \frac{2F}{r_o w(\phi_o + \sin\phi_o)} \tag{1-9}$$

The angular velocity of the input shaft when the weights make initial contact with the drum may be found by setting the square bracket in equation (1-6) equal to zero. Substitution of $\omega = 2\pi n/60$, where n is in rpm, followed by solving the resulting expression for n, yields

$$n = \frac{\pi}{30}\sqrt{\kappa \frac{g}{r_c(\beta) + \delta}(1 + \eta)} \tag{1-10}$$

The role of parameters β and λ in equation (1-5) upon force F, equation (1-3), and therefore upon $p_{\max}$, equation (1-9) and the speed at which they first contact the drum are shown in Figures 2(a) through (d).

Observe that the variation of the pressure, and hence the force, that each weight exerts against the drum is a linear function of parameter λ and that it becomes a nearly linear function of β, and hence of r_i, for β greater than about 0.3. The dependence of the width of each weight, however, becomes increasingly nonlinear as β increases and as λ decreases. The rotational speed for initial contact is also nearly linear for $\beta < 0.6$, especially for the larger values of λ.

Example

Design a centrifugal clutch to provide a torque of 2400 N-m when the rotational speed reaches 870 rpm using sector weights having the geometry shown in Figure 3(a). Preferred characteristics are that initial contact between weights and drum occur at between 220 and 230 rpm and that the width of the weights be less than 30 cm. Assume a lining coefficient of friction of 0.35 and design for an inside drum radius (minus the lining thickness) of 15 cm, a displacement δ of 3 mm for the segments to contact the drum, and a static deflection of 1 mm. The segments are to be made from an iron alloy having a nominal density of 7880 kg/m^3, and a safety factor of 3.5 is mandated. Hold

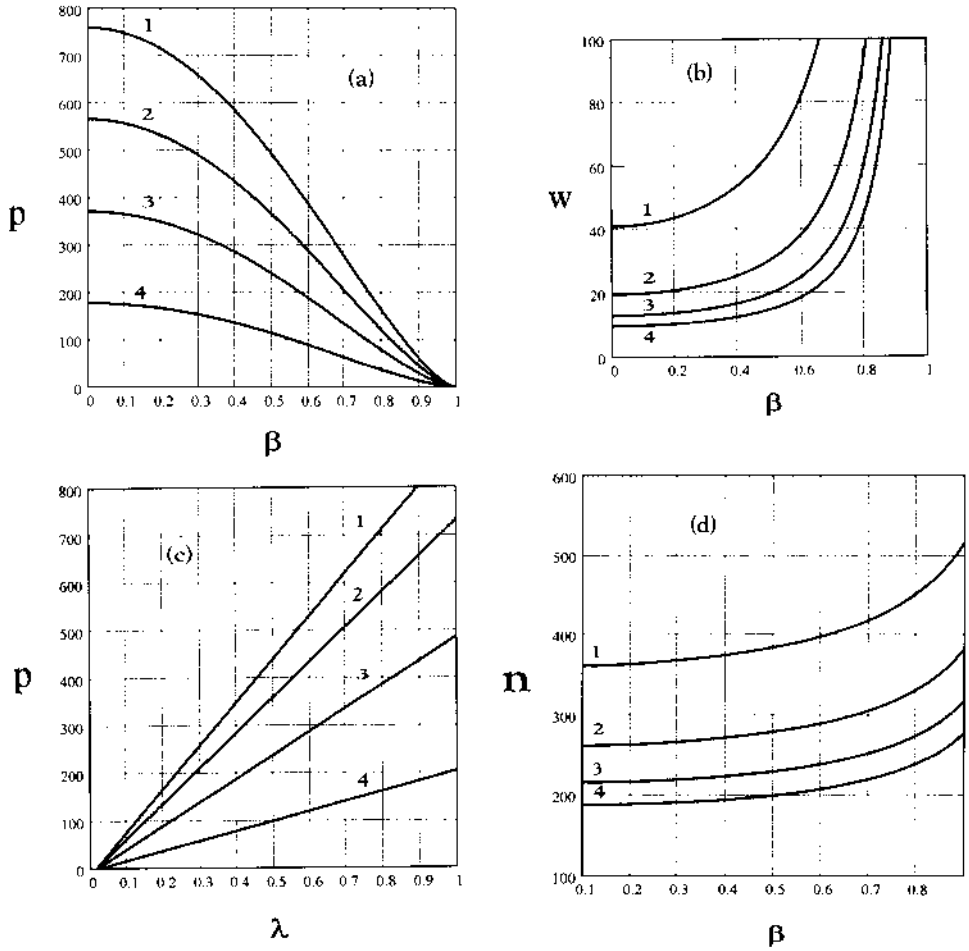

FIGURE 2 (a) Variation of pressure (kPa) with β for $\lambda = 0.2, 0.4, 0.6$, and 0.8 for curves 1, 2, 3, and 4, respectively. (b) Variation of width (cm) with β for $\lambda = 0.2, 0.4, 0.6$, and 0.8 for curves 1, 2, 3, and 4, respectively. (c) Variation of pressure (kPa) with λ for $\beta = 0.2, 0.4, 0.6$, and 0.8, respectively. (d) Variation of contact speed (rpm) with λ for $\beta = 0.2, 0.4, 0.6$, and 0.8 for curves 1, 2, 3, and 4, respectively.

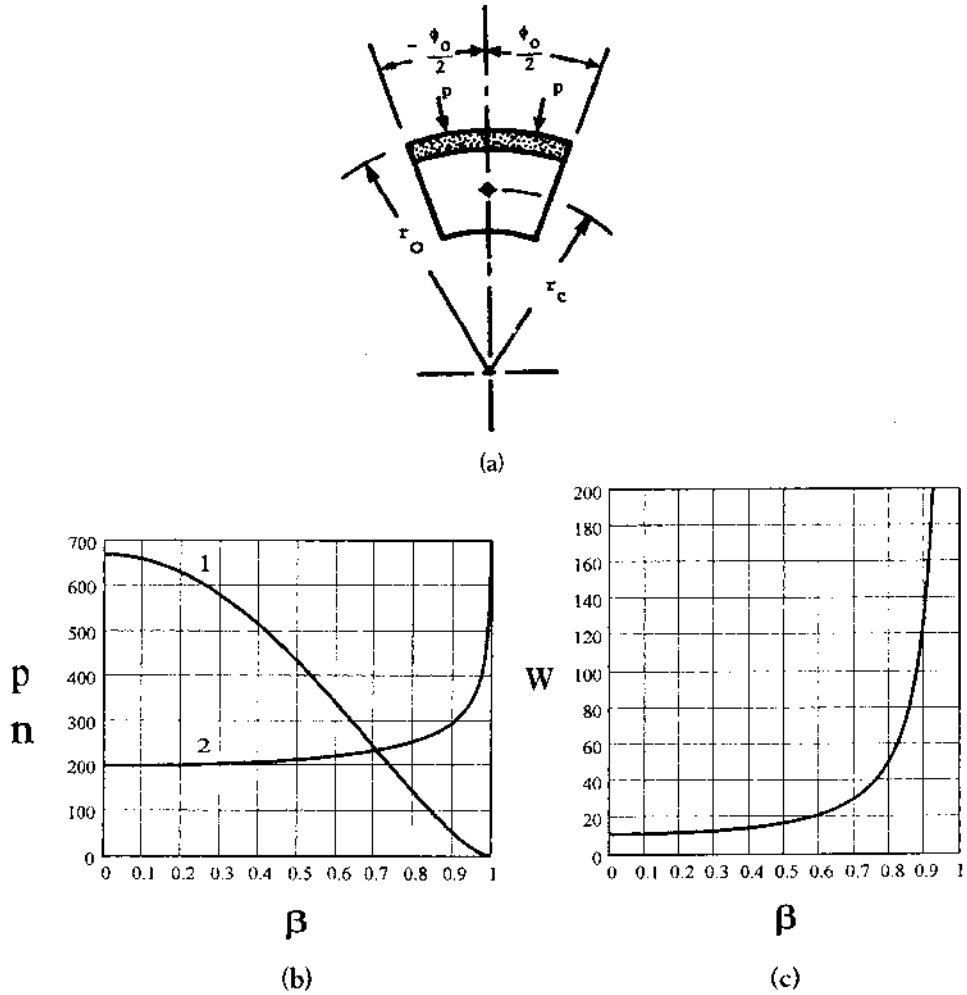

FIGURE 3 (a) Sector cross section. (b) Curve 1: pressure P (kPa) vs. β; Curve 2: initial contact speed n (rpm) vs. β. (c) Sector width w (cm) vs. β.

the weights against their rest position with a force 1.2 times their weight. Maximum lining pressure of less than 440 kPa is preferred.

Because the lining pressure on a segment decreases with angle θ from the centerline of that segment according to equation (4-2), use six weights to get a greater force transfer, each subtending an angle $\phi_n = 42°$.

Begin the design process by plotting pressure p, contact speed n, and width w against β by substituting the following values into equations (1-1) through (1-3), (1-5) through (1-7), and (1-9).

$T = 24,000$ N-m $\quad r_o = 150$ m $\quad \gamma = 7880$ kg/m^3 $\quad n = 870$ rpm $\quad c = 0.50$

$\delta = 0.003$ m $\quad \delta_s = 0.001$ m $\quad \kappa = 1.2$ $\quad \phi_o = 42°$ $\quad \mu = 0.35$

$\eta = 3 \quad N = 6 \quad \lambda = \dfrac{1}{\sqrt{2}} \quad g = 9.8067$ m/sec^2

These plots are shown in Figure 3(b) and (c).

Figure 3(b) shows that an initial contact speed between 220 and 230 rpm may be had for β between 0.6 and 0.7, Figure 3(c) shows that the corresponding width of the sector would be less than 30 cm. Substituting $\beta = 0.65$ into equation (1-10) yields $n = 226.59$ rpm, which is within the desired range. This is close enough to the preferred value of 225 rpm for manual iteration of β to find that

$$n = 225.001 \text{ rpm} \qquad \text{at} \qquad \beta = 0.6367$$

The width of each weight and the maximum lining pressure corresponding to $\beta = 0.6357$ are found to be

$$w = 23.8 \text{ cm} \qquad \text{and} \qquad p_{\max} = 304 \text{ kPa}$$

by substitution into equations (1-7) and (1-9), respectively. The required spring constant may be found by substituting from equation (1-1) into equation (1-2) to get

$$k = wc\phi_o r_o^2 \gamma \frac{g}{\delta_s} \kappa (1 - \beta^2) \tag{1-11}$$

Substitution into this expression yields

$$k = 1366 \text{N/mm}$$

II. ONE-WAY CLUTCH: THE SPRING CLUTCH

Wiebusch gave the first description of this clutch, shown in Figure 4, in 1930 [1]. As may be soon from the figure, it consists of a helical spring snugly, wrapped about both the input and output hubs, parts 1 and 3 in Figure 4, but is attached to neither of them. If the input hub tends to turn in the direction that causes the helix to tighten, the increased friction between the spring and hubs tends to resists any further relative rotation. Relative rotation in the

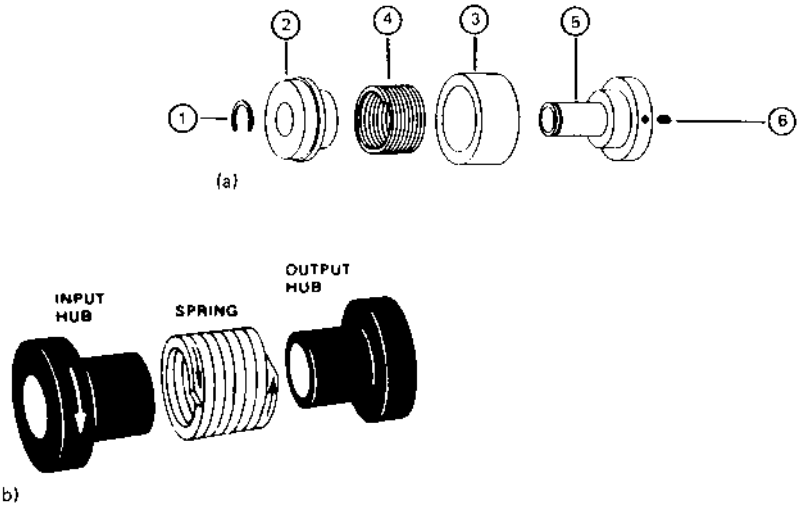

FIGURE 4 Spring clutch and its components. (Courtesy Warner Electric Brake & Clutch Co., South Beloit, IL.)

other direction, however, tends to loosen the helix, and relative rotation may proceed with only a relatively small restraint by the spring clutch.

Although Wahl [2] appears to have derived a more accurate expression for the torque that may be transmitted, T_t, agreement between the Wiebusch theory and experiment seems to be close enough to justify use of the simpler relationship, which is

$$T_t = Elr_h\left(\frac{1}{R_2} - \frac{1}{R_1}\right)\left(e^{2\pi N\mu} - 1\right) \tag{2-1}$$

in terms of the elastic modulus E of the spring material, the moment of area I of the spring wire in bending, the radius R_1 of the neutral surface of the wire in helix 4 in Figure 4 when it is free of external load, the radius R_2 of the wire when the helix is in tight contact with hubs 1 and 5 in the figure, and the number of turns N on one hub if both hubs have the same number of turns. If both hubs do not have the same number of turns, N is the smaller of the two. The friction coefficient is represented by μ, and r_h denotes the hub radius.

Wiebusch found that the torque T_u in the unwinding direction was approximately equal to

$$T_u = Elr_h\left(\frac{1}{R_2} - \frac{1}{R_1}\right)\left(1 - e^{-2\pi N\mu}\right) \tag{2-2}$$

Equation (2-1) obviously holds for a torque less than that which corresponds to the maximum force than can be carried by the spring wire at yield. Kaplan and Marshall [3] have indirectly suggested that the limiting torque satisfies the inequality

$$T_{\max} \leqslant bt^2 \frac{1.05}{2r_h}\left(R_1 - R_2 - \frac{t}{2}\right) \tag{2-3}$$

for rectangular wire whose dimension in the radial direction is t and whose dimension in the axial direction of the helix is b.

III. OVERRUNNING CLUTCHES: THE ROLLER CLUTCH

These clutches are designed to transmit torque from shaft A to shaft B when shaft A tends to rotate faster than shaft B but to disengage when shaft B rotates faster than A. Details of four designs that accomplish this are shown in Figure 5, which shows that the clutch consists of two concentric races, in which one is circular and the other consists of a series of cams, with a roller under, or above, each cam. Relative rotation which wedges the rollers between the narrow portion of the cam and the circular surface of the other race forces both races to rotate together, while relative rotation in the opposite direction frees the rollers and allows the two races to rotate at different angular rates.

In particular, if the cams are cut in the outer race and tapered in the direction shown in Figure 5(a), (b), and (c), rotation of the inner race in the clockwise direction will cause the rollers to wedge themselves between the two races so that the outer race must also rotate in the clockwise direction, that is, when

$$\omega_i > \omega_o$$

If the outer race is then accelerated to a rotational speed greater than that of the inner race so that

$$\omega_o > \omega_i$$

the roller will move to the larger ends of the cam and the outer race is free to accelerate to a speed greater than that of the inner race. The sequence just described is, for example, that used in starting gas turbines with an electric motor to get them up to operating speed, at which point the turbine accelerates under its own power and disengages the starter motor, which is then shut off.

If the cam surface is cut in the inner race and tapered as shown in Figure 5 (d), clockwise rotation of the outer race will drive the inner race whenever

$$\omega_o > \omega_i$$

Acceleration of the inner race in the clockwise direction will cause the clutch to disengage whenever

$$\omega_o < \omega_i$$

as is obvious from the taper geometry. These clutches are said to be free-wheeling or overrunning when the relative rotation of the race is such that no torque is transmitted from one to the other.

From the geometry of Figures 5 it follows that the torque transmitted to a roller and a convex race is limited by the maximum contact stress that can be sustained along the line of contact (actually, a narrow strip after the surfaces have deformed slightly) between the roller and the race with the smaller radius of curvature.

$$\sigma_{xx} = \frac{-2F}{\pi^2 a}(a^2 + 2x^2 + 2z^2)\frac{z}{a}\Psi - 2\pi\frac{z}{a} - 3xz\Phi + \mu(2x^2 - 2a^2 - 3z^2)\Phi + 2\mu\pi\frac{x}{a} + 2\mu(a^2 - x^2 - z^2)\frac{x}{a}\Psi \tag{3-1a}$$

$$\sigma_{zz} = -\frac{2F}{\pi^2 a}z(a\Psi - x\Phi + \mu z\Phi) \tag{3-1b}$$

$$\sigma_{xz} = -\frac{2F}{\pi^2 a}\left[z^2\Phi + \mu(a^2 + 2x^2 + 2z^2)\frac{z}{a}\Psi - 2\pi\mu\frac{z}{a} - 3\mu xz\Phi\right] \tag{3-1c}$$

away from the contacting surfaces and by

$$\sigma_{xx} = -\mu\frac{4F}{\pi a}\left[\frac{x}{a} - \left(\frac{x^2}{a^2} - 1\right)^{1/2}\right], \quad x \geqslant a$$

$$= -\frac{2F}{\pi a}\left[\left(1 - \frac{x^2}{a^2}\right)^{1/2} + 2\mu\frac{x}{a}\right], \quad -a \leq x \leq a \tag{3-2a}$$

$$\sigma_{xx} = -\mu\frac{4F}{\pi a}\left[\frac{x}{a} - \left(\frac{x^2}{a^2} - 1\right)^{1/2}\right], \quad x \leqslant -a$$

If a finite element analysis program with contact stress capability is not available, the pertinent stress components may be estimated from an analysis by Smith and Liu [4] for the contact (Hertzian) stresses between two parallel

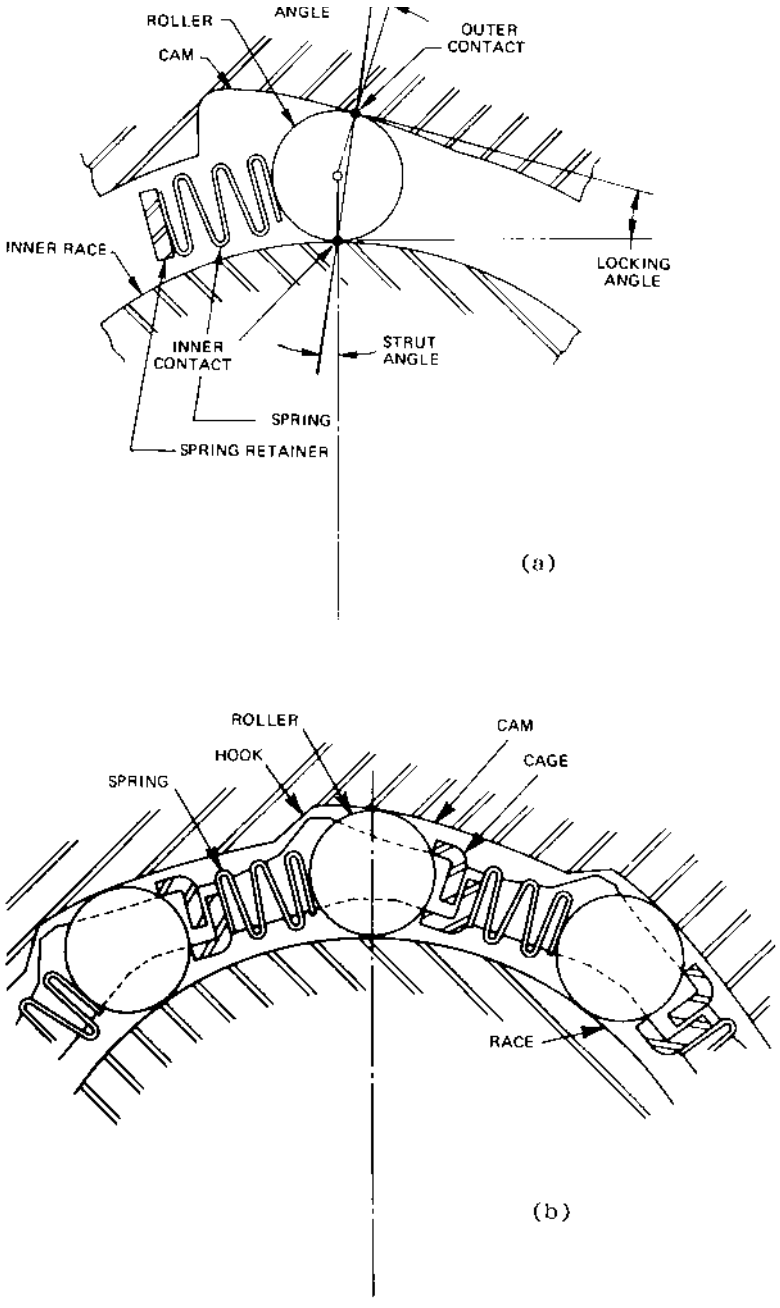

FIGURE 5 Typical roller clutch configurations. (a) Outer cam type of roller one-way clutch diagram. (b) Caged roller type of clutch diagram (hook-type cam). (c) Loose roller type of clutch diagram (leg-type cam). (d) Inner can type of roller one-way clutch diagram. (Reprinted with permission; © 1984 Society of Automotive Engineers, Inc.)

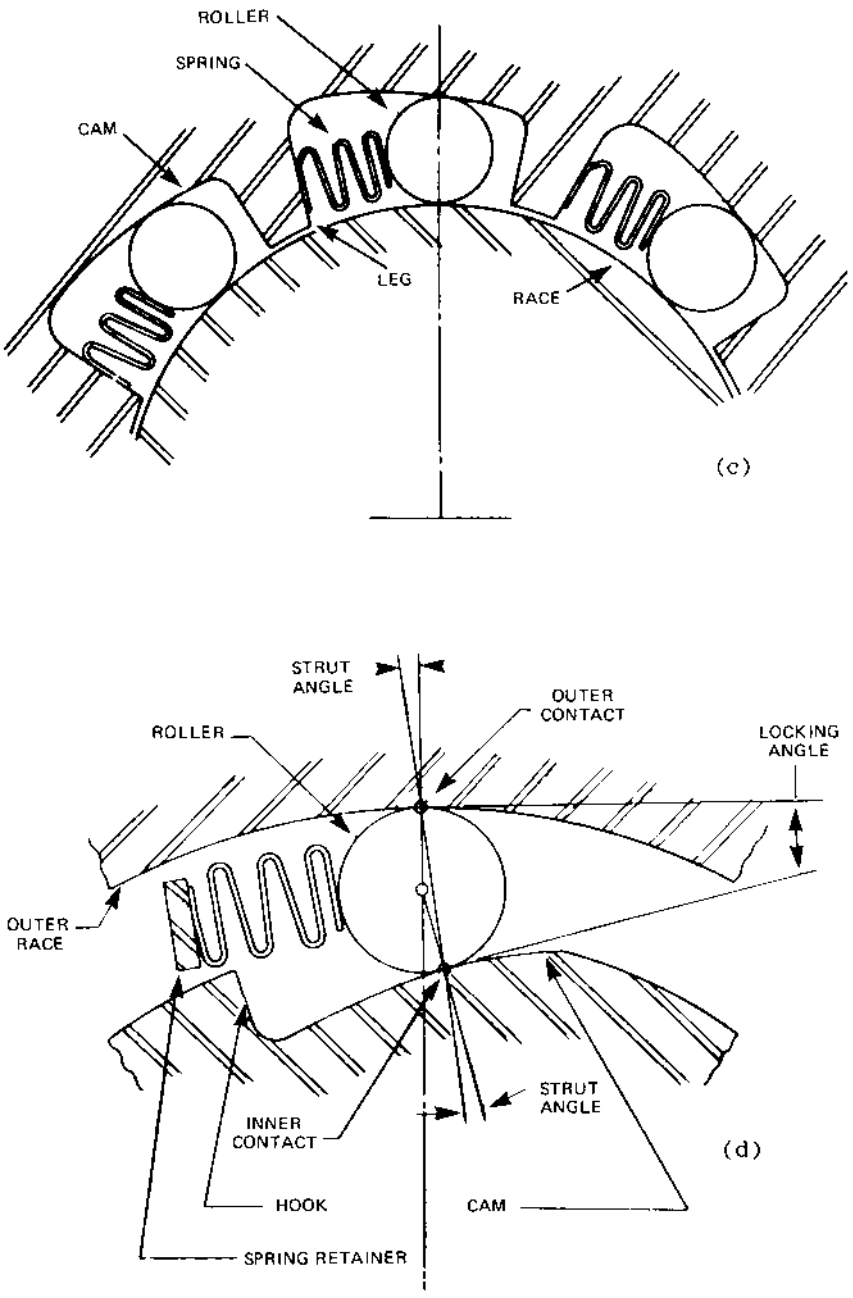

FIGURE 5 Continued.

cylinders, such as between the rollers and the inner races in Figure 6 (a), (b), and (c).

$$\begin{aligned}\sigma_{zz} &= -\frac{2F}{\pi a}\left(1-\frac{x^2}{a^2}\right)^{1/2}, \qquad -a \leqslant x \leqslant a \\ &= 0, \qquad x \leqslant -a,\ x \geqslant a\end{aligned} \tag{3-2b}$$

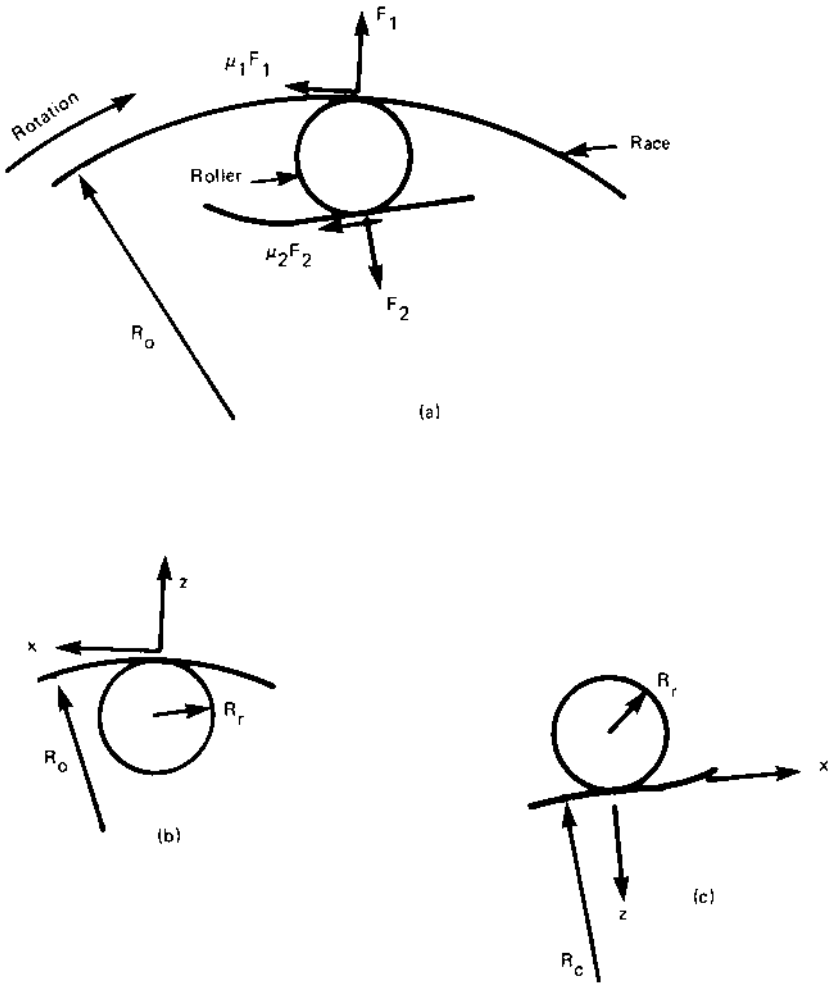

FIGURE 6 Forces on cam and race in an overrunning roller clutch.

$$\sigma_{xz} = -\frac{2F}{\pi a}\mu\left(1 - \frac{x^2}{a^2}\right)^{1/2}, \quad -a \leqslant x \leqslant a$$
$$= 0, \qquad x \leqslant -a,\ x \geqslant a \tag{3-2c}$$

on the contacting surface. For larger values of μ the maximum stress is on the surface and for smaller values it lies below the surface. Quantities Φ and Ψ in equation (3-1) are defined by

$$\Phi = \frac{\pi}{k_1\phi}\left[1 - \left(\frac{k_2}{k_1}\right)^{1/2}\right] \qquad \Psi = \frac{\pi}{k_1\phi}\left[1 + \left(\frac{k_2}{k_1}\right)^{1/2}\right]$$

$$\phi = \left(2\frac{k_2}{k_1}\right)^{1/2}\left[\left(\frac{k_2}{k_1}\right)^{1/2} + \frac{k_1 + k_2 - 4a^2}{2k_1}\right]^{1/2}$$

where

$$k_1 = (a + x)^2 + z^2 \qquad k_2 = (a - x)^2 + z^2$$

$$a = 2\left(\frac{E}{\pi}\frac{\dfrac{1 - v_1^2}{E_1} + \dfrac{1 - v_2^2}{E_2}}{\dfrac{1}{r_1} + \dfrac{1}{r_2}}\right)^{1/2}$$

Quantities v_1, v_2, r_1, r_2, E_1, and E_2 refer to the Poisson ratios, radii, and Young's moduli of the components in contact, i.e., a roller and the outer race or a roller and the inner race. Since the trios of quantities v_1, r_1, E_1 and v_2, r_2, E_2 enter symmetrically into the expression for a, either trio may be associated with a roller and the other trio associated with the inner race. Coordinates x and z lie in the circumferential and radial directions, respectively, and quantity a represents the half-width of the contact area measured in the circumferential direction, hence the inclusion of F in the definition of a. Loading force per unit length in the axial direction between a race and a roller is denoted by F. One misprint and one apparent misprint have been corrected by the author in reproducing equations 4 and 12 in Ref. 4 in the preceding set of equations.

Maximum compressive stress at the surface between a roller and a concave race is given by

$$\sigma_{zz} = \frac{-1}{\pi}\left[F\frac{\left(\dfrac{1}{r_1} - \dfrac{1}{r_2}\right)}{\left(\dfrac{1 - v_1^2}{\pi E_1} + \dfrac{1 - v_2^2}{\pi E_2}\right)}\right]^{1/2} \tag{3-3}$$

from Ref. 5.

Insertion of the force F used to calculate the previous stresses into equation (3-3) will give the torque transferred to the outer ring as

$$T = FNl[r_1 + r_3(l + \cos\alpha)](\sin\alpha + \mu\cos\alpha) \tag{3-4}$$

in terms of the angle α between F_1 and the direction of F_2, the length/of each of the rollers, the number of rollers, N, the radius r_1, and the radius of a roller, r_3.

Forces acting on a roller as it is wedged between the inner and outer races are shown in Figure 7. Summing forces in the direction of F_1 yields

$$F_2\cos\alpha + \mu_2 F_2\sin\alpha = F_1 \tag{3-5}$$

and summing forces perpendicular to the direction of F_2 yields

$$F_2\sin\alpha = \mu_2 F_2\sin\alpha + \mu_1 F_1 \tag{3-6}$$

From Figure 7 we note that the magnitude of the force transmitted to the outer race is given by $F_2(\sin\alpha - \mu_2\cos\alpha)$. This force would reach its maximum and the shear stress on the roller and outer race would vanish if only a normal force acted between a roller and the outer race or, more precisely, the

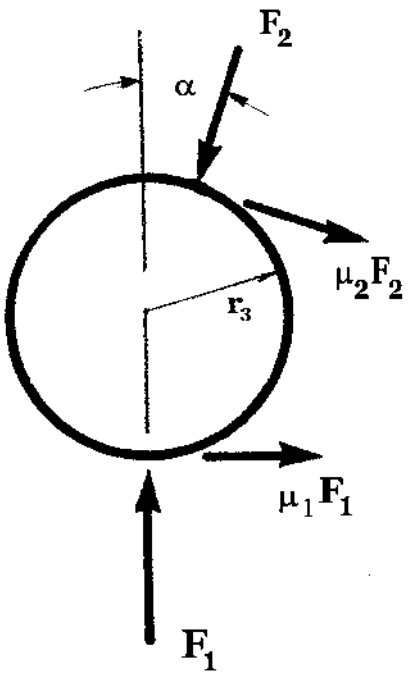

FIGURE 7 Forces acting on a roller wedged between an outer cam and and the inner race.

internal cams on the outer ring. To find the requirement for this condition to be true, set $\mu_2 = 0$ in equations (3-5) and (3-6) to get the equations that hold when only a normal force. F_2, acts between a cam and a roller, as in Figure 7. Substitute the value of F_1 from equation (3-5) into equation (3-6). The result is $\sin \alpha = \mu, \cos \alpha$, or

$$\tan \alpha = \mu_1 \tag{3-8}$$

Therefore lubrication of the races (races and cams) and rollers not only reduces wear on the contacting surfaces, but also reduces the angle of the outer cams, for which equation (3-8) is satisfied.

Example

Is it possible to produce a roller clutch to provide a torque of 950 ft-lb that has an inner race no more than 5 in. in diameter and that has a roller length equal to or less than 1.8 in.? Assume that the roller and races are made from a material whose working stress should be no more than 100,000 psi in either tension or shear and that its Young's modulus is that of steel.

Assume Poisson's ratio of 0.3, a friction coefficient of 0.34, and a Young's modulus of 3×10^7 psi. Since the circumference of a 5-in. diameter race is 15.71 in., initially select 10 rollers with 0.50-in. diameters and assume a strut angle of 9°. Let the initial trial contact length of each roller be 1.8 in.

First solve equation (3-5) for F to find $F = 36.776$ lb/in. Substitute $F = 36.776$ lb/in. into equations (3-1) and (3-2) and the definitions of the parameters to get $a = 7.925 \times 10^{-4}$ in., so the contact width is from $x = -0.0079$ in. to $x = 0.00079$ in. Values of k_1 and k_2 are $k_1 = 2.389 \times 10^{-6}$ in.^{2} and $k_2 = 1.676 \times 10^{-6}$ in.^{2}, and parameters Φ and Ψ are given by $\Phi = 1.610 \times 105$ in.$^{-2}$ and $\Psi = 1.826 \times 10^6$ in.$^{-2}$. After calculating the foregoing stress component at the surface and at 0.001 in. below the surface, we find that the largest tensile stress for the points calculated on the surface was 78,060 psi at $x = -0.001$, the largest shear stress was 43,560 psi at the center of the contact area and the largest compressive stress was −78,060 psi at $x = 0.001$ in. At $z = 0.001$ in. below the surface, all of the direct stresses calculated were compressive, the largest being $\sigma_{xx} = 1{,}642{,}000$ psi at $x = -0.001$ in. The largest stress found was $\sigma_{xx} = 98{,}140$ psi at $x = -0.00018$ in., just outside of the contact region at $z = 0.001$ in. Equation (3-3) gave a compressive stress $\sigma_{xx} = -26{,}530$ psi at the surface of the cam on the outer ring.

IV. OVERRUNNING CLUTCHES: THE SPRAG CLUTCH

A representative sprag clutch is shown in Figure 8. These clutches are also direction depenent, but they differ from the roller clutches in that sprags are used rather than circular cylindrical rollers. Sprags are cylinders whose cross section, as shown in Figure 9, is designed to allow them (1) to engage and

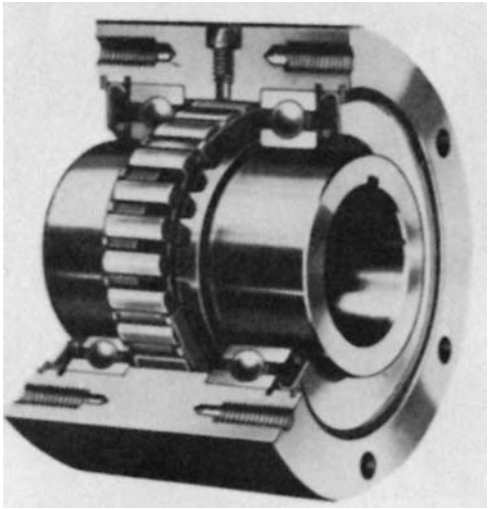

FIGURE 8 Overrunning sprag clutch. (Courtesy Dana Corp., Inc., Toledo, OH.)

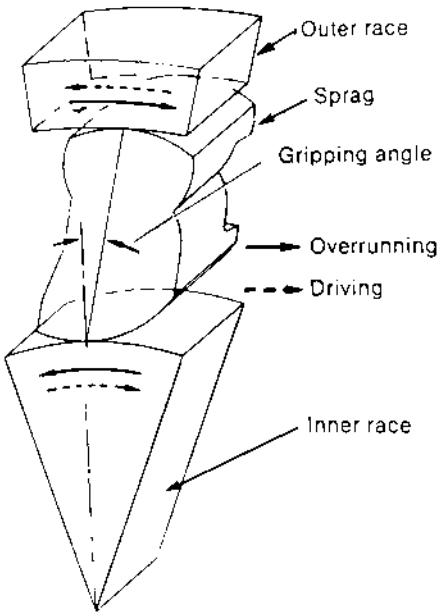

FIGURE 9 Conventional sprag and a sector of its inner and outer races.

disengage in a fraction of a turn and (2) to provide a larger radius of curvature along the contact line between the sprag and the races than would be possible if complete circular cylinders were used. Placing more sprags between the inner and outer races increases the torque by increasing N in equation (3-5) while increasing the radius of curvature reduces the $(1/R_1 - 1/R_2)$ term in equations (3-1) and (3-2) and thereby reduces the contact stress for a given value of F, which permits an increase in the magnitude of F in equation (3-5) for a given stress level in each race. These comments also apply to sprags whose cylindrical surface has been cut by intersecting planes, as in Figure 10, to further increase N, the number of contacting sprags.

Some sprags are designed to respond to centrifugal forces as well as frictional forces, so that as the rotational speed of the faster race increases, the sprags rotate under the influence of the centrifugal force and break contact with one of the races, thereby reducing wear and drag.

Sprags designed to respond only to friction are often termed conventional sprags, while those which are designed to respond to both friction and to an increase in speed are termed either throw-out or throw-in sprags, depending on whether they disengage from the inner or outer race at the lift-off speed.

Conventional sprags and three installation variations are shown in Figure 11. The energizing spring in all three configurations is to hold the sprags in a position to become engaged as soon as conditions permit, while the cages, shown in Figure 11(a) and (c), are to space the sprags apart to reduce

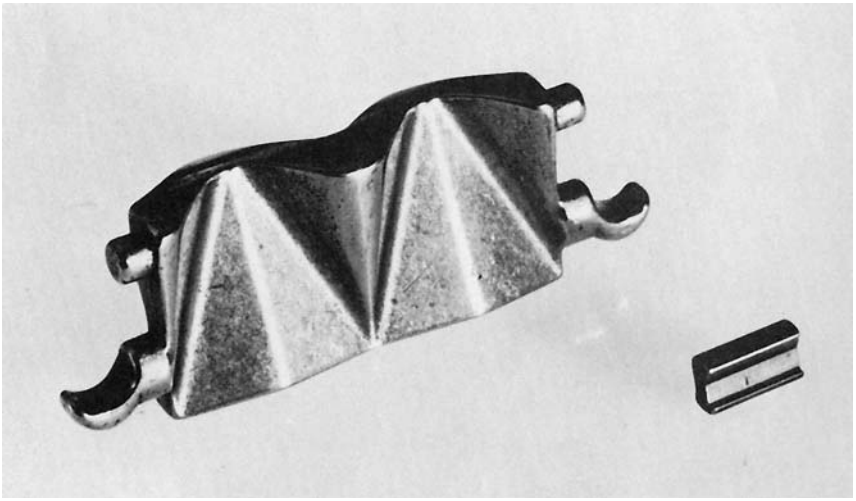

FIGURE 10 Modified sprag design for closer packing. (Courtesy Georg Muller of America, Inc., Schaumburg IL.)

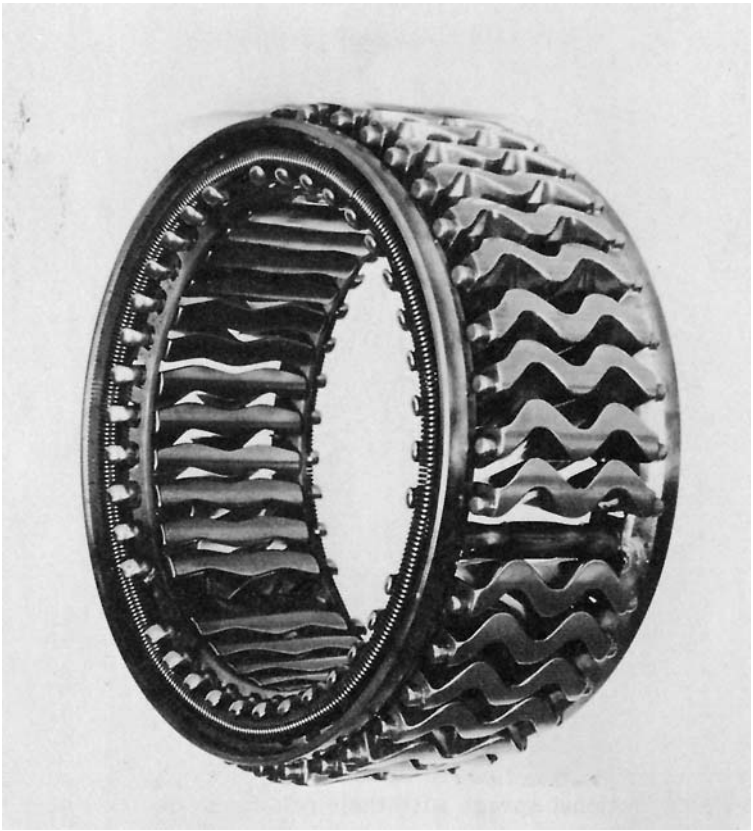

FIGURE 10 Continued.

friction between them and permit faster engagement. Double cages are used to allow the first few sprags that make contact to force the remaining sprags into contact as these first ones assume a more radial orientation and thus cause angular rotation of one cage relative to the other. They may be used with external connections to force disengagement before the driven race reaches a speed greater than that of the driving race. Full complement configurations, represented by Figure 11(b), are used for larger torsional loads, while the single- and double-cage configurations are for smaller loads and faster response.

One version of an overrunning throw-out sprag is shown in Figure 12, in which the cage rotates with the outer race. The small projection at the left of each sprag in this figure not only aids in moving the center of gravity to provide a rotational moment due to the centrifugal force, but acts as a stop

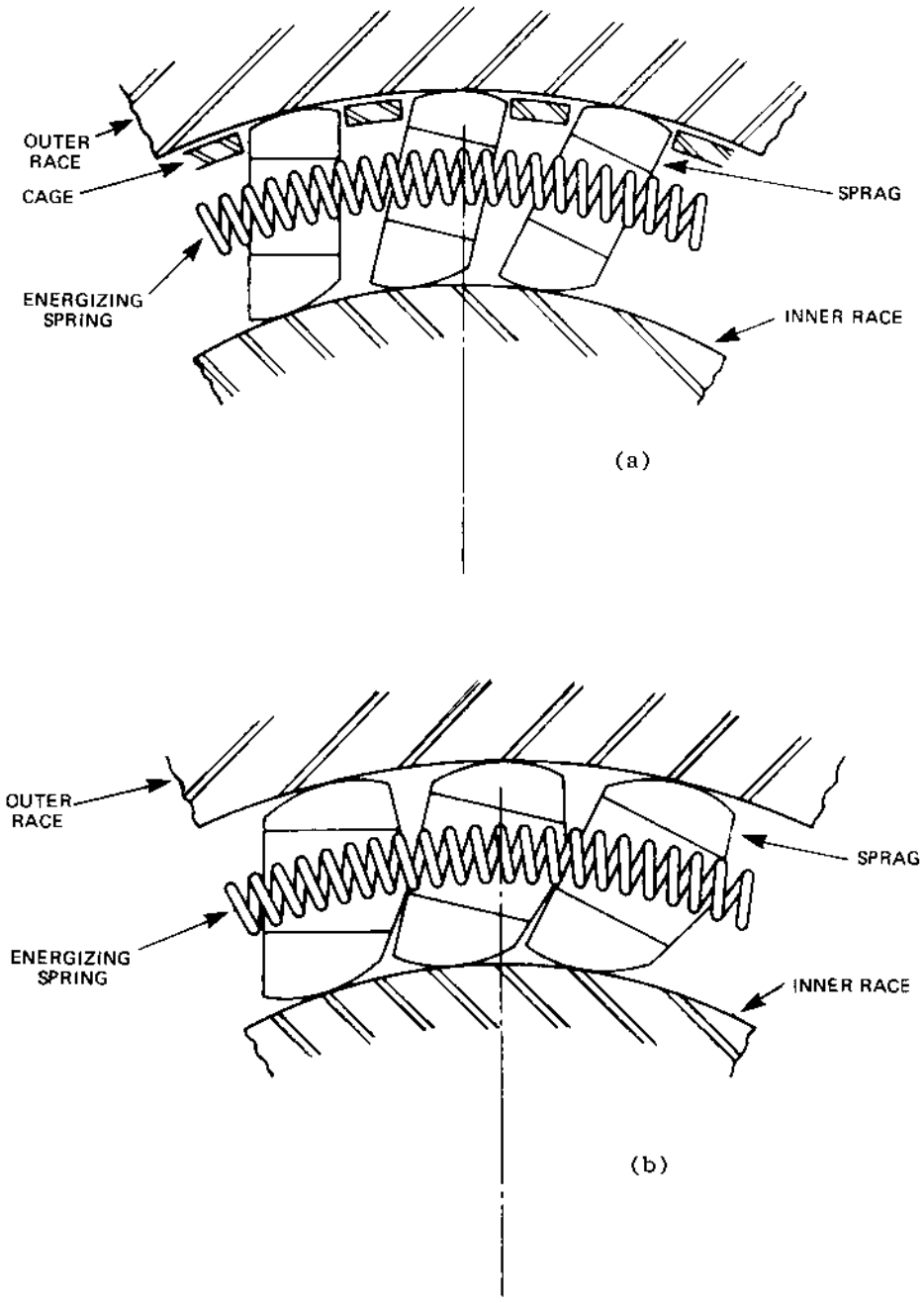

FIGURE 11 Conventional sprags with their retaining springs and cages. (a) Typical single-cage one-way clutch diagram. (b) Typical full-complement sprag one-way clutch diagram. (c) Typical double-cage sprag one-way clutch diagram. (d) Sprag one-way clutch diagram. (Reprinted with permission; © 1984 Society of Automotive Engineers, Inc.)

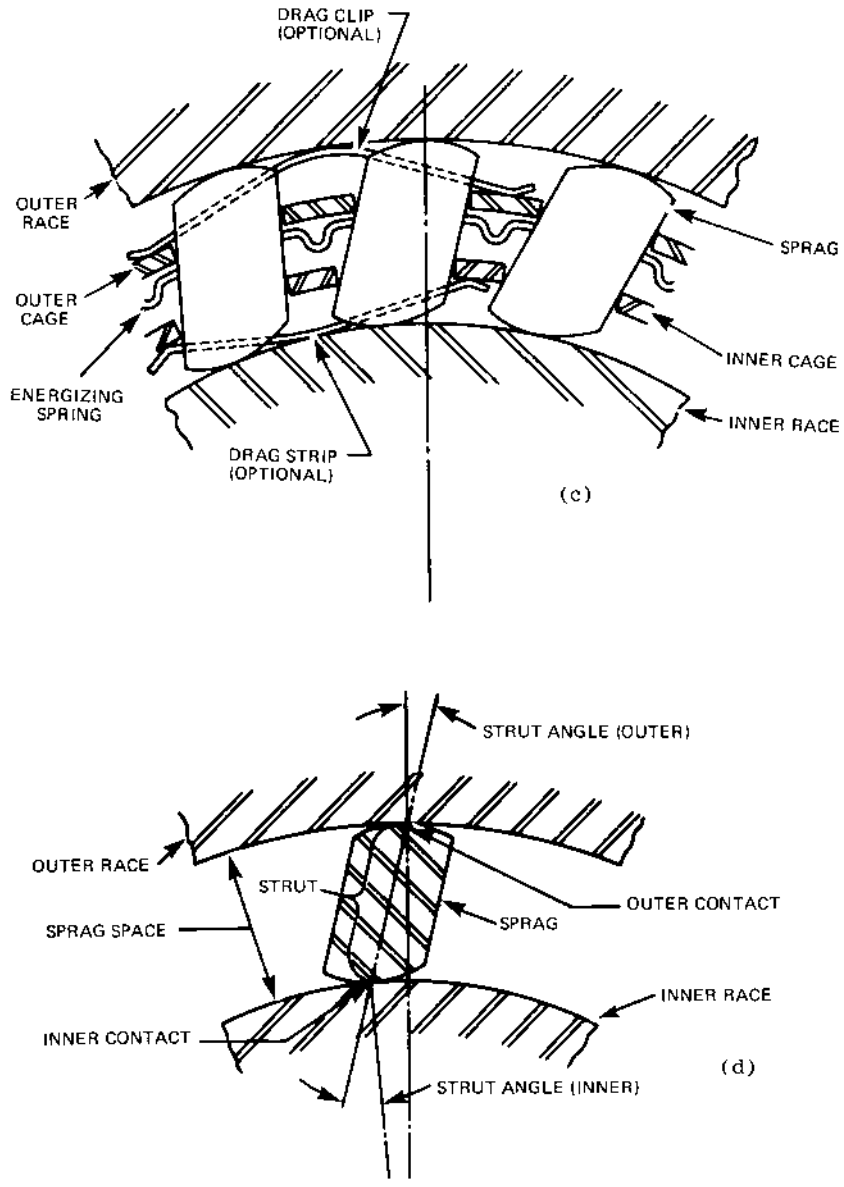

FIGURE 11 Continued.

to prevent sprag rollover under clutch overload conditions, as pictured in Figure 12(c). Springs between the cage and the sprags, not shown in these figures, may be selected to control the lift-off speed.

One manufacturer of throw-in clutches uses a sprag and spring design, as shown in Figure 13, where the sprag retainer, or cage, moves with the inner race so that as the speed of that race increases, the centrifugal force acting on the center of mass of the sprag, which lies to the right of the pivot, causes the

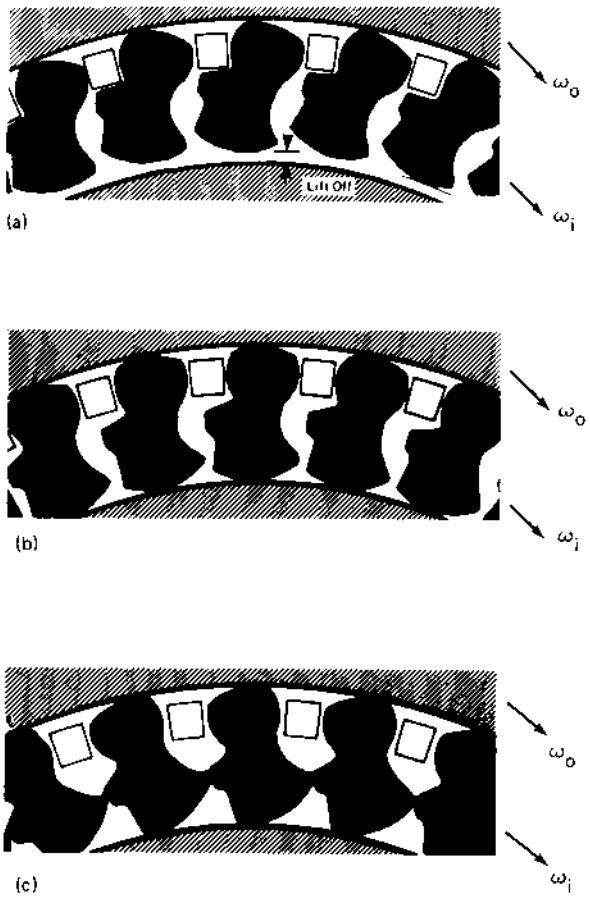

FIGURE 12 Throw-out sprags with antiroller rails; *C*/*T* designates centrifugal throw-out: (a) High RPM–*C*/*T* overrunning: $\omega_o > \omega_i$. (b) Regular engagement condition: $\omega_o = \omega_i$. (c) Overload-imposed conditions: $\omega_o = \omega_i$. (Courtesy Dana Corp., Toledo, OH.)

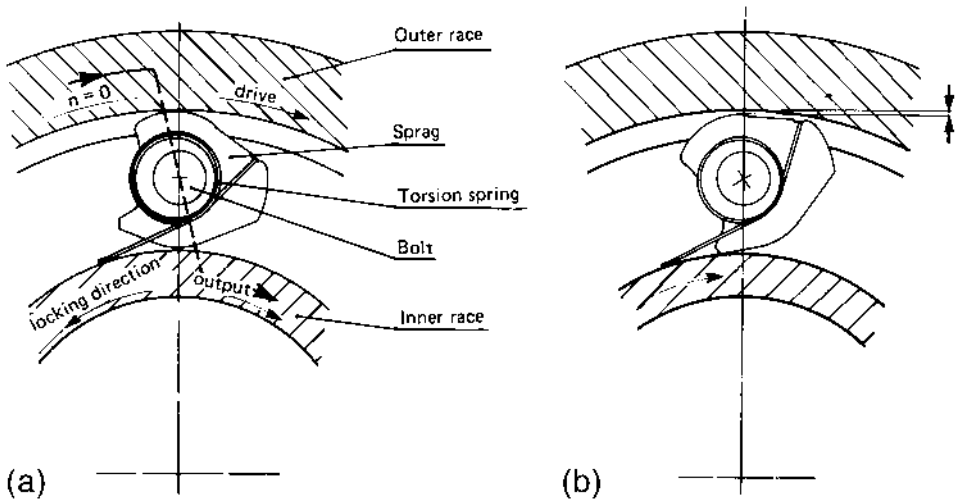

FIGURE 13 Throw-in sprag configuration and spring. (a) Regular engagement. (b) Centrifugal throw-in engagement.

sprag to rotate in a counterclockwise direction and lose contact with the outer race. As the speed of the inner race decreases, the spring causes the sprag to rotate in the clockwise direction so that it will again make contact with the outer race.

Returning now to the conventional sprag profile, let A and B denote the contact points on the profile of a sprag, as shown in Figure 14, let the line between A and B termed the *strut*, and let α represent the angle subtended by the strut at the center of the clutch. Let r_o and r_i represent the radii of the outer and inner races, respectively, let μ_o and μ_i denote the corresponding coefficients of friction, and let F_o and F_i refer to the associated normal forces. In these terms,

$$\mu_o F_o r_o - \mu_i F_i r_i = 0 \tag{4-1}$$

is the moment equilibrium equation of the sprag about the axis of rotation of the clutch. Summing forces in the direction of the friction force at A gives

$$\mu_o F_o + F_i \sin\alpha - \mu_i F_i \cos\alpha = 0 \tag{4-2}$$

as the equilibrium condition in that direction. Substitution for F_o in equation (4-2) from equation (4-1) yields

$$\frac{r_i}{r_o} = \cos\alpha - \frac{1}{\mu_i}\sin\alpha \tag{4-3}$$

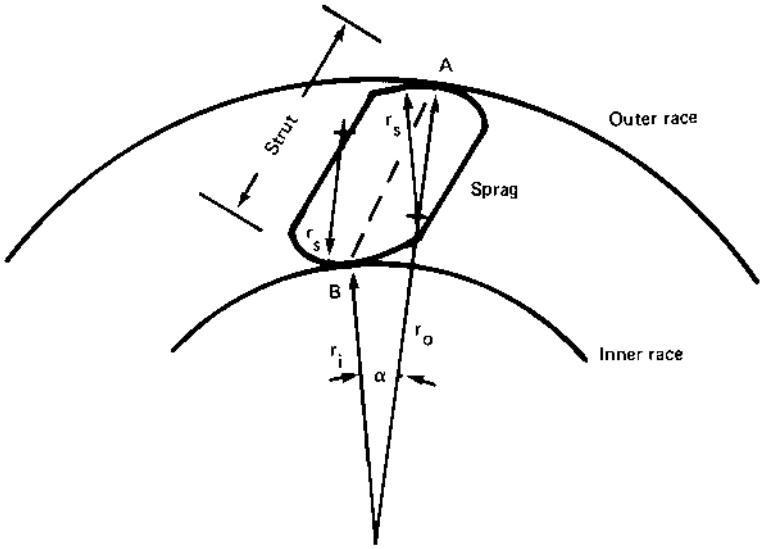

FIGURE 14 Sprag and race geometry: r_i = radius of inner race; r_o = radius of outer race; r_s = radius of sprag contact surface (commonly the arc of a circle or of a logarithmic spiral).

as a guide in selecting angle α. The value of sin α may be found by substituting for cos α from equation (4-3) and substituting into the trigonometric identity

$$\sin^2 \alpha + \cos^2 \alpha = 1$$

and then solving for sin α from the quadratic formula to give

$$\sin \alpha = \frac{r_i}{r_o} \frac{\mu_i}{1+\mu_i^2} \left\{ \left[1 + (1+\mu_i^2)\left(\frac{r_o}{r_1} - 1\right)\right]^{1/2} - 1 \right\} \tag{4-4}$$

Forces F_o and F_i are related to the torque according to

$$F_i \leq \frac{T}{\mu_i - N - r_i} \tag{4-5}$$

and, from the equilibrium equations for the sprag,

$$F_o = \frac{\mu_i \frac{r_o}{l} \sin(\alpha) - \cos\left(\alpha \sin\left(\frac{r_o}{l}\sin(\alpha)\right)\right)}{\mu_o \sin\left(\alpha + \alpha\sin\left(\frac{r_o}{l}\sin(\alpha)\right)\right) - \cos\left(\alpha + \alpha\sin\left(\frac{r_o}{l}\sin(\alpha)\right)\right)} \tag{4-6}$$

$$> \frac{T}{\mu_o N r_o}$$

in which l is the length from A to B in Figure 14. These values of r_s and r_i may be substituted into equations (3-1) and (3-2) and values of r_s and r_o substituted into equation (3-3) or into a finite element program for contact stresses at the inner and outer radii, to find the minimum radius of curvature r_s, shown in Figure 14, that will give a permissible stress for these sprag profiles for the inner race (IR) and for the outer races (OR). Different radii may be selected for contact stresses at the IR and OR for the sprag configurations shown in Figure 11.

Sprag overrunning clutches have speed envelopes within which they can operate as designed. Although these envelopes have the same general shape, the nature of the envelope in the third quadrant (that to the left of the vertical axis and below the horizontal axis) may vary as shown in Figures 15 and 16 for sprag clutches. Recommended operating speeds lie between the upper curve, which is the upper boundary of the envelope, and the 45° diagonal, which is the lower boundary of the envelope. In both figures the upper curved arrow in each quadrant depicts the direction of rotation of the outer race in that quadrant, the lower curved arrow in each quadrant indicates the direction of rotation of the inner race in that quadrant, and the inclined line between the

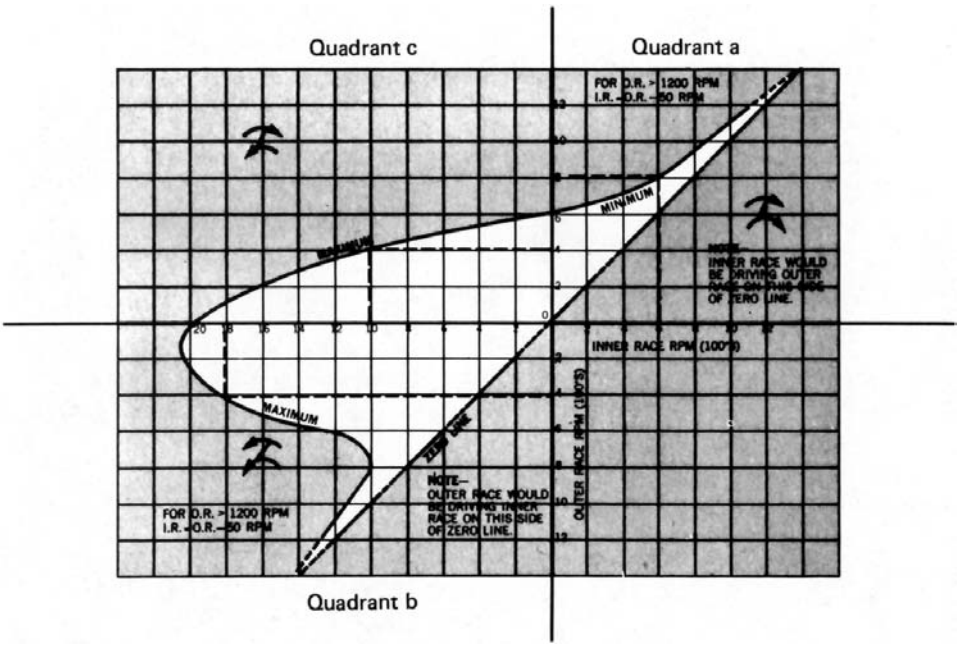

FIGURE 15 Relative overrun speed envelope showing the directions of rotation and the strut angle. (Courtesy Dana Corp., Toledo, OH.)

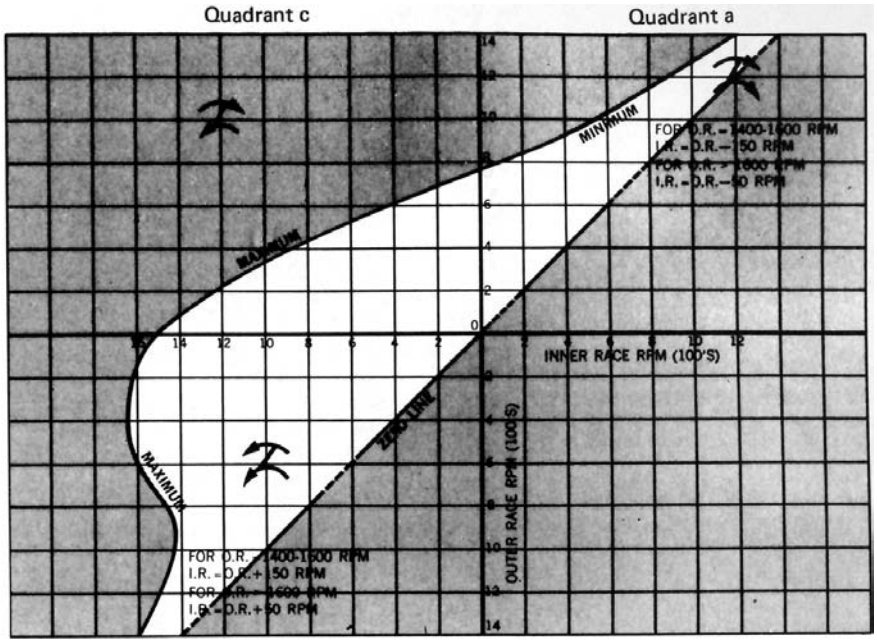

FIGURE 16 Relative overrun speed envelope showing representative variation between models. (Courtesy Dana Corp., Toledo, OH.)

curved arrows indicates the direction of the strut. In all cases clockwise rotation is taken as positive.

No curved arrows are shown in the fourth quadrant because in that quadrant the IR rotation is positive, the OR rotation is negative, and the strut thrust angle is such that one will always drive the other, so that no overrunning is possible. No overrunning will occur at points in the first quadrant below the diagonal because in this region the OR rotates more slowly than the IR but the strut angle is such that the IR cannot overrun the OR. Similar reasoning regarding the third quadrant will show that the OR cannot override the IR.

Rotational combinations corresponding to points above and/or to the left of the envelope in the first and second quadrants are not recommended even though overrunning is possible in these regions because at these higher rotational speeds of the OR it tends to accelerate the IR in the first quadrant and decelerate it in the second quadrant. Similarly, rotational speeds corresponding to points below and/or to the left of the envelope in the third quadrant, where overrunning in possible, are not recommended because these IR speeds tend to accelerate the OR. As noted in Figure 15, at OR speed in

excess of 1200 rpm in the first and third quadrants, the IR rotational speed tends to be only 50 rpm less than the OR speed.

V. TORQUE LIMITING CLUTCH: TOOTH AND DETENT TYPES

Although tooth clutches, as pictured in Figure 17, are usually used for positioning one shaft relative to the other, they may, in an emergency, also serve as overload detent clutches, because their torque is limited by the axial force

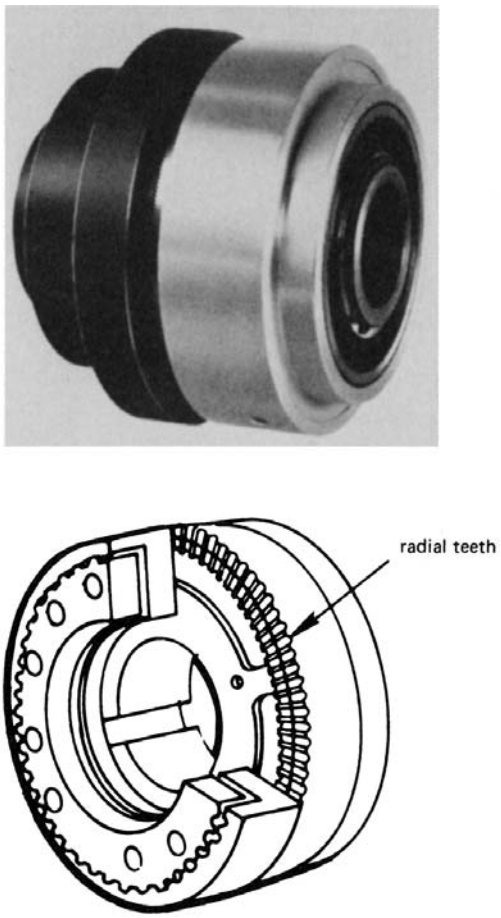

FIGURE 17 Tooth clutch for shaft positioning.

holding the toothed jaws together. From Figure 18 we find that the tangential, F_t, and normal, F_n, forces are given by

$$F_t = N \sin \zeta + \mu N \cos \zeta \tag{5-1}$$

and

$$F_n = N \cos \zeta - \mu N \sin \zeta \tag{5-2}$$

from which it follows that the ratio F_t/F_n, the ratio of the tangential load to the axial load, becomes

$$\frac{F_t}{F_n} = \frac{\sin \zeta + \mu \cos \zeta}{\cos \zeta - \mu \sin \zeta} \tag{5-3}$$

which may be simplified to read

$$\frac{F_t}{F_n} = \tan(\zeta + \beta) \tag{5-4}$$

if β is defined to be

$$\beta = \tan^{-1} \mu \tag{5-5}$$

The maximum torque that a tooth clutch with wedge-shaped teeth can transmit may be estimated from

$$T = N r_k F_n \tan(\zeta + \beta) \tag{5-6}$$

where N is the number of teeth and r_k is the radius from the axis of the clutch to the circle that passes through the center of the teeth in Figure 17.

Clutches designed specifically as overload release clutches remain engaged only if the transmitted torque is less than a prescribed critical value. Once that value is exceeded, the clutch is disengaged and remains disengaged until it is manually reset. Several versions will be considered here.

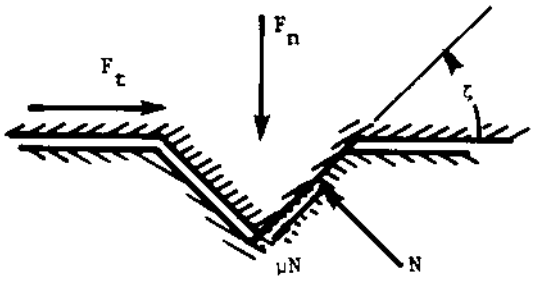

FIGURE 18 Forces acting on a single wedge tooth. (Courtesy Horton Mfg. Co., Minneapolis, MN, and Machine Design, Penton Press, Cleveland, OH.)

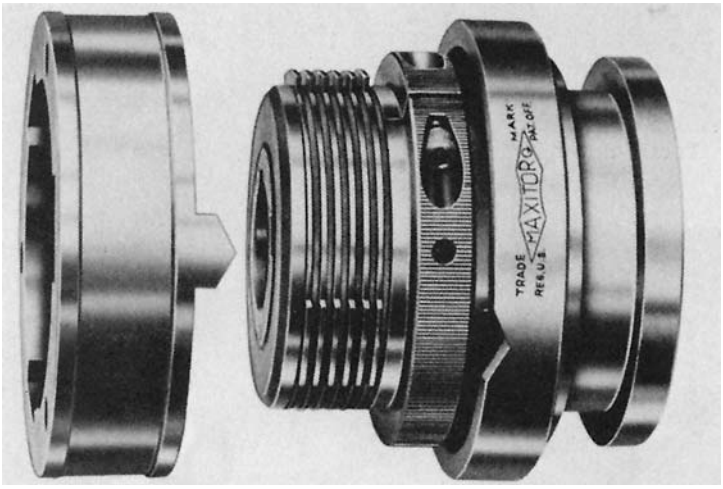

FIGURE 19 Overload release clutch using clutch plates and wedge-shaped release cam. (Courtesy of Carlyle Johnson Machine Co., Manchester, CT.)

The first is shown in Figure 19. Torque is transferred by means of clutch plates that are alternately keyed to the driver ring on the left and to the clutch body that is concealed by the clutch plates and is enclosed by the sleeve on the right in this figure. A collar on the input shaft (not shown) is bolted to the driver ring and the clutch body is keyed to the output shaft. Pressure between clutch plates is exerted by the adjusting ring that is shown just to the right of the clutch plates. A trio of levers that lie between that clutch body and the outer sleeve that extends to the right of the adjusting ring hold the adjusting ring in place when the race on the sleeve engages the cam on the driver ring. An overload causes the clutch plates to slip, which in turn allows the cam on the driver ring to push against the race on the sleeve and cause it to move axially to the right to disengage internal levers that maintain clamping pressure on the clutch plates. Until the clutch is reset the torque transfer drops to 1% of the rated torque with no ratcheting. Rated torque capability for clutches of this type from this manufacturer range from 20 lbs ft. to 2400 lbs ft., depending upon size.

A second style of overload clutch may employ spring-loaded rollers (or balls) held in sockets attached to one plate such that the rollers rest in pockets in the other, as shown in Figure 20. These rollers will remain in the pockets as long as the tangential force between plates is satisfies

$$F_t \leqslant F_k \frac{\cos\zeta + \mu(1 + \sin\zeta)}{\sin\zeta - \mu(1 + \cos\zeta)} \tag{5-7}$$

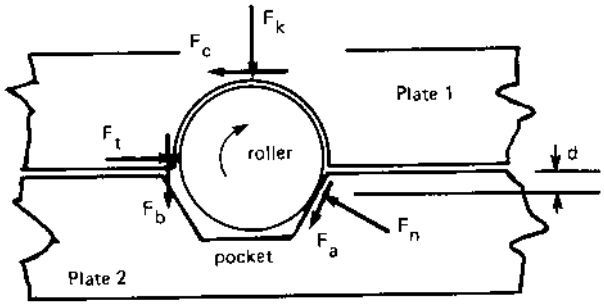

FIGURE 20 Forces on a typical roller or ball in a detent clutch using one or more such elements. The spring-loading mechanism is replaced by F_k and F_c.

where F_k is the spring force on the ball, F_t is the lateral force on the ball, μ is the coefficient of friction, and ς is the angle between the detent wall and the vertical. This relation may be derived by taking moments about the instantaneous center at the contact between the roller and the pocket in Figure 20.

Torque transmitted by the clutch may be written as

$$T = F_t RN \tag{5-8}$$

where R is the radius from the center of the balls to the axis of rotation of the disk on which they are mounted and N is the number of spring-and-ball assemblies on the disk. When equality holds in equation (5-7), substitution for F_t from equation (5-8) into equation (5-7) yields that the spring force must satisfy

$$F_k = \frac{T}{NR} \frac{\sin\zeta - \mu(1 + \cos\zeta)}{\cos\zeta + \mu(1 + \sin\zeta)} \tag{5-9}$$

Most, if not all, detent overload clutches use something similar to the geometry shown schematically in Figure 20, in which the detents are in one plate and the spring-loaded balls and their retainers are mounted on the other plate. Immediately after an overload occurs, the balls are pushed from their detents and pop into and out of adjacent detents until either the rotation is stopped or the overload is removed. Consequently it is often recommended that they be used on shafts that rotate at less than 500 rpm to reduce damage to both the balls and the detents. The transmitted torque after the balls are pushed from their detents may be about 5% of the rated torque of the clutch. Ball and detent arrangements in clutches where indexing (maintaining a constant angular relation between input and output shafts) after an overload is not required usually are arranged in axial symmetry in order to reduce shaft vibration and noise.

Many manufacturers of ball and detent overload clutches designed for applications where indexing is important are reluctant to display the particular designs used to achieve automatic indexing after an overload is removed. The following description of a detent arrangement is offered, therefore, only to show that a simple detent layout is possible that can provide automatic indexing. It is based upon the observation that without axial symmetry of the detent positions there should be only one relative position between mating disks where all of the balls in one disk fit into all of the detents in the other disk so that the clutch can transmit its rated torque.

An example of one possible configuration is that shown in Figure 21, in which each detent subtends an angle of 10° from the center of the disk and all eight detents lie in a circle about the center of the disk so that they all contribute equally to the total torque.

Three disadvantages of this arrangement are: (1) the balls slam into and out of the detents when the disks rotate relative to one another in the overload condition; (2) the plates must have masses either added or removed to establish dynamic balance; and (3) shaft speed should usually be no more than 500 rpm. During overloading, this type of clutch may transmit a small fluctuating torque that could be of the order of 5–13% of the rated torque until the overload is removed. The compensating advantage is that after the overload is removed, the clutch automatically reindexes to the proper position.

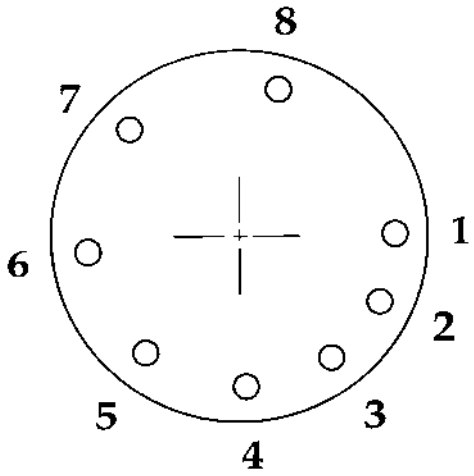

FIGURE 21 Detent positions for an indexing ball and detent overload clutch.

Detent center locations, and that of the mating detent balls, shown in Figure 21, are arranged according to the angular positions shown in the following table. Addition of $\Delta\theta^\circ$ shown in the top row above detent number 1 to the value of θ° just above detent number 1 gives θ° for detent number 2, and so on.

$\Delta\theta^\circ$		25	30	35	40	45	50	60	75	
θ°	0	25	55	90	130	175	225	285	360
Detent number	1	2	3	4	5	6	7	8	1

This detent arrangement could be improved. That is because in each rotation of the disk fitted with the spring-loaded ball assembly relative to the disk in which the detents are cut there are three relative orientations where two ball-and-detent pairs engage. In those three instances the torque may momentarily jump to 25% of the rated torque rather than to the 12.5% that may occur when only one ball-and-detent pair engages.

To elaborate, if the ball-and-detent pairs are numbered in the clockwise direction when viewed from the driving plate to the driven plate, as in Figure 21, we find that during clockwise rotation of the driving plate relative to the driven plate three instances occur wherein two ball-and-detent pairs are engaged before the plates reindex. The first instance occurs when balls 8 and 3 engage detents 1 and 5. This is because the angular separation between detents 8 and 3 is the same as that between detents 1 and 5. In particular, from the preceding table of the angular positions of the ball-and-detent pairs and the angular separation between centers we find

75° between detents 8 and 1
25° between detents 1 and 2
30° between detents 2 and 3
130° between detents 8 and 3

and that the angular separation between detent centers 1 and 5 is given by

25° between detents 1 and 2
30° between detents 2 and 3
35° between detents 3 and 4
40° between detents 4 and 5
130° between detents 1 and 5

The second instance occurs when balls 8 and 1 engage detents 1 and 5, where ball centers 8 and 1 are separated by 75° and detent centers 3 and 4 are

separated by 35° and 4 and 5 are separated by 40° for a combined separation of 75°. The third and last instance is when balls 7 and 1 engage detents 4 and 7. Placing ball-detent pairs at different radii eliminates engagement except at the index position, but those ball and detent locations at smaller radii transmit less torque.

VI. TORQUE LIMITING CLUTCH: FRICTION TYPE

Torque limiting friction clutches are another version of overload clutches. They differ from those considered in the previous sections in that the transmitted torque does not drop sharply from the rated torque. Instead, the

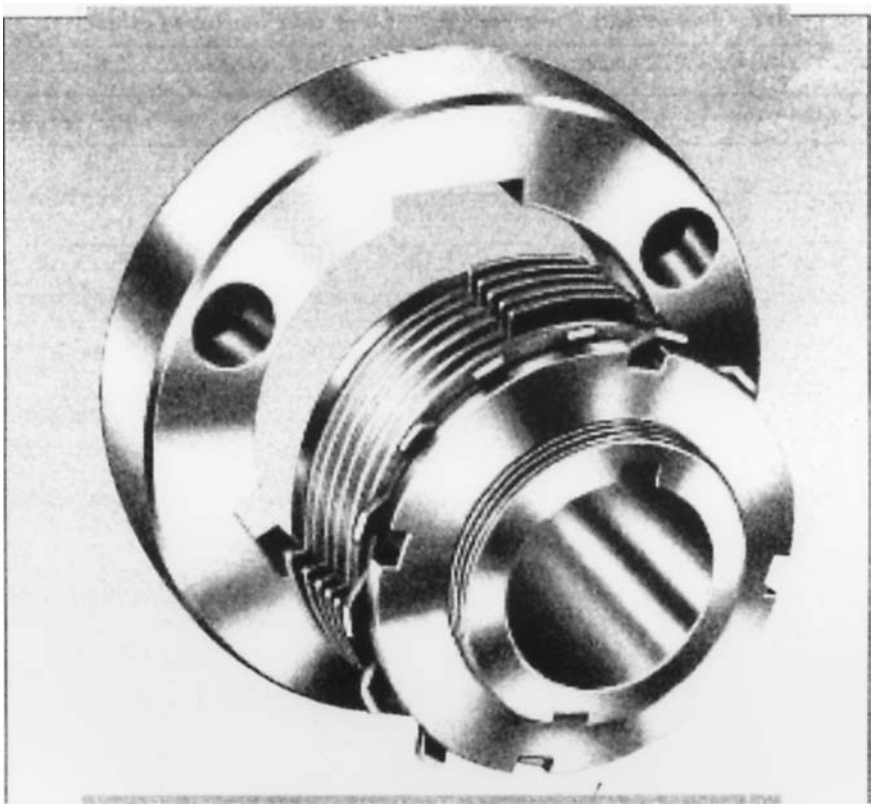

FIGURE 22 Torque limiting clutch. From the Carlyle Johnson Machine Co., Bolton, CT, Web page on the Thomas Register Web site.

transmitted torque does not exceed a preset value regardless of the speed or of the torque imposed by the driven unit. The clutch simply slips when its preset torque is exceeded. A torque limiting friction clutch, as shown in Figure 22, consists of a series of spring-loaded clutch plates in which greased alternate steel and bronze plates are keyed to the input and output sections of the clutch. Spring loading to set the torque limit is accomplished by controlling the spring force on the plates by means of the adjusting nut at the right-band end of the clutch hub. Grease sealed within the hubs provides a lubricant between the clutch plates, and it is the viscous characteristics of the grease that are used to determine the torque characteristics of the clutch, i.e., the slope of the curves in Figure 23. Consequently, a variety of torque characteristics are available. Torque limits are a linear function of the spring compression, also as illustrated in Figure 23 for a particular grease.

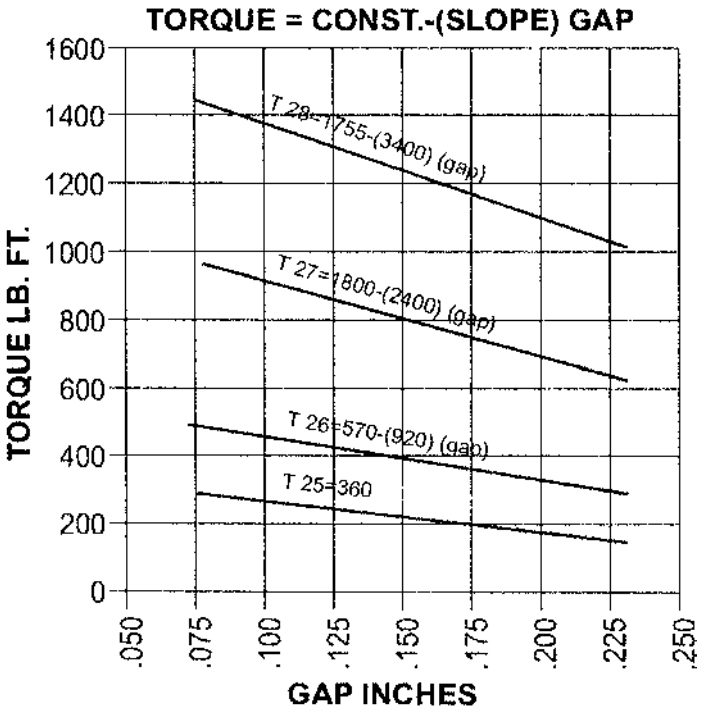

FIGURE 23 Torque as a function of the adjustable gap for the models noted. From the Carlyle Johnson Machine Co., Bolton, CT, Web page on the Thomas Register Web site.

Torque capabilities of models similar to that shown in Figure 22 range from 0 to 10 lb-ft up to 0 to slightly over 1400 lb-ft.

VII. NOTATION

A	area (l^2)
a	factor in Hertzian (contact) stress formulas (l)
b	width, rectangular wire (l)
c	correction factor (1)
E	elastic modulus (Young's Modulus) ($ml^{-1}t^{-2}$)
F	force (mlt^{-2})
g	acceleration due to gravity (lt^{-2})
l	moment of area (l^4)
k	spring constant (mt^{-2})
m	mass (m)
N	number, an integer (1)
n	angular velocity in revolutions per minute, rpm (t^{-1})
p	pressure ($ml^{-1}t^{-2}$)
R,r	radius (l)
r_o	radius to a centroid (l)
T	torque (ml^2t^{-2})
t	time (t) or wire thickness (l)
W	weight (mlt^{-2})
w	width (l)
x,z	cartesian coordinates (l)
α	angle (1)
β	ratio of radii (1)
γ	mass density (ml^{-3})
δ	displacement (l)
ζ	safety factor (1)
η	displacement ratio (1)
θ	angle (1)
κ	spring multiplication factor (1)
λ	centroid parameter (1)
μ	friction coefficient (1)
ν	Poisson's ratio (1)
σ	stress ($ml^{-1}t^{-2}$)
Φ	factor in Hertzian (contact) stress formulas (l^{-2})
ϕ	angle (1) and intermediate parameter in Hertzian stress formulas
Ψ	factor in Hertzian (contact) stress formulas (l^{-2})
γ	angular velocity in radians (t^{-1})

VIII. FORMULA COLLECTION

Maximum pressure, centrifugal clutch:

$$p_{\max} = \frac{2F}{r_o w(\phi_o + \sin\phi_o)}$$

Torque, centrifugal clutch:

$$T = \gamma r_o F = \mu\gamma w r_o \, NA\left[(r_o + \delta)\omega^2 - g\kappa(1+\eta)\right] \quad \eta = \delta/\delta_s$$

Torque, spring clutch, winding direction:

$$T_t = Elr_h\left(\frac{1}{R_2} - \frac{1}{R_1}\right)(e^{2\pi\mu N} - 1)$$

Torque, spring clutch, unwinding direction:

$$T_u = Elr_h\left(\frac{1}{R_2} - \frac{1}{R_1}\right)(1 - e^{-2\pi\mu N})$$

Maximum torque, spring clutch, based on wire dimensions:

$$T_{\max} \leqslant bt^2 \frac{1.05}{2r_h}\left(R_1 - R_2 - \frac{t}{2}\right)$$

Normal plus tangential contact stress, away from surface:

$$\sigma_{xx} = -\frac{2F}{\pi^2 a}\left[(a^2 + 2x^2 + 2z^2)\frac{z}{a}\Psi - 2\pi\frac{z}{a} - 3xz\Phi \right.$$
$$\left. + 2\pi\mu\frac{x}{a} + \mu(2x^2 - 2a^2 - 3z^2)\Phi + 2\mu(a^2 - x^2 - z^2)\frac{x}{a}\Psi\right]$$
$$\sigma_{zz} = -\frac{2F}{\pi^2 a} z(a\Psi - x\Phi + \mu z\Phi)$$
$$\sigma_{xz} = -\frac{2F}{\pi^2 a}\left[z^2\phi + \mu(a^2 + 2x^2 + 2z^2)\frac{z}{a}\Psi - 2\mu\pi\frac{z}{a} - 3\mu xz\Phi\right]$$

Normal plus tangential contact stress, on surface:

$$\sigma_{xx} = -\mu\frac{4F}{\pi a}\left[\frac{x}{a} - \left(\frac{x^2}{a^2} - 1\right)^{1/2}\right] \qquad \text{for } x \geqslant a$$
$$= -\frac{2F}{\pi a}\left[\left(1 - \frac{x^2}{a^2}\right)^{1/2} + 2\mu\frac{x}{a}\right] \qquad \text{for } -a \leqslant x \leqslant a$$
$$\sigma_{xx} = -\mu\frac{4F}{\pi a}\left[\frac{x}{a} + \left(\frac{x^2}{a^2} - 1\right)^{2}\right] \qquad x \leqslant -a$$

$$\sigma_{zz} = -\frac{2F}{\pi a}\left(1 - \frac{x^2}{a^2}\right)^{1/2} \qquad \text{for } -a \leqslant x \leqslant a$$
$$= 0 \qquad \text{for } x \leqslant -a,\ x \geqslant a$$

where

$$\Phi = \frac{\pi}{k_1 \phi}\left[1 - \left(\frac{k_2}{k_1}\right)^{1/2}\right] \qquad \Psi = \frac{\pi}{k_1 \phi}\left[1 + \left(\frac{k_2}{k_1}\right)^{1/2}\right]$$

$$\phi = \left(2\frac{k_2}{k_1}\right)^{1/2}\left[\left(\frac{k_2}{k_1}\right)^{1/2} + \frac{k_1 + k_2 - 4a^2}{2k_1}\right]^{1/2}$$

$$k_1 = (a + x)^2 + z^2 \qquad k_2 = (a - x)^2 + z^2$$

$$a = 2\left(\frac{F_r}{\pi}\frac{\dfrac{1 - v_1^2}{E_1} - \dfrac{1 - v_2^2}{E_2}}{\dfrac{1}{r_1} + \dfrac{1}{r_2}}\right)^{1/2}$$

for all previous normal and tangential contact stresses (i.e., modified Hertzian stresses).

Hertzian stress, outer ring, cam:

$$\sigma_{zz} = \frac{-1}{\pi}\left[F\frac{\dfrac{1}{r_1} - \dfrac{1}{r_2}}{\left(\dfrac{1 - v_1^2}{\pi E_1} + \dfrac{1 - v_2^2}{\pi E_2}\right)}\right]^{1/2}$$

Radial force, centrifugal clutch:

$$F = \gamma w A\left[(r_c + \delta) - g\kappa\frac{\delta + \delta_s}{\delta_s}\right]$$

Torque, overload detent clutch:

$$F_t = \frac{T}{NR}\frac{\sin\zeta - \mu(1 + \cos\zeta)}{\cos\zeta + \mu(1 + \sin\zeta)}$$

Spring constant, centrifugal clutch:

$$k = wc\phi_o^2 r_o^2 \gamma \frac{g}{\delta_s}\kappa(1 - \beta^2)$$

REFERENCES

1. Wiebusch, C. F. (1939). The spring clutch. *Journal of Applied Mechanics*. Vol. 6:A103–A108.
2. Wahl, A. M. (1940). Discussion of the spring clutch. *Journal of Applied Mechanics*. Vol. 7:A89–A91.
3. Kaplan, J., Marshall, D. (1956). Spring clutches. *Machine Design*. Vol. 28:107–111.
4. Smith, J. O., Liu, C. K. (1953). Stresses due to tangential and normal loads on an elastic solid with application to some contact stress problems. *Journal of Applied Mechanics*. Vol. 20:157–168.
5. Timoshenko, S. P., Goodier, J. N. (1970). *Theory of Elasticity*. NY: McGraw-Hill Book Co., pp. 417–418.
6. Poritsky, H. (1950). *Journal of Applied Mechanics*. Vol. 17:191.